SUPPLEMENTARY INFORMATION

Supplementary Figures

Supplementary Table

Supplementary Experimental Procedures

Supplementary References

Supplementary Figure 1 (related to Figure 2)

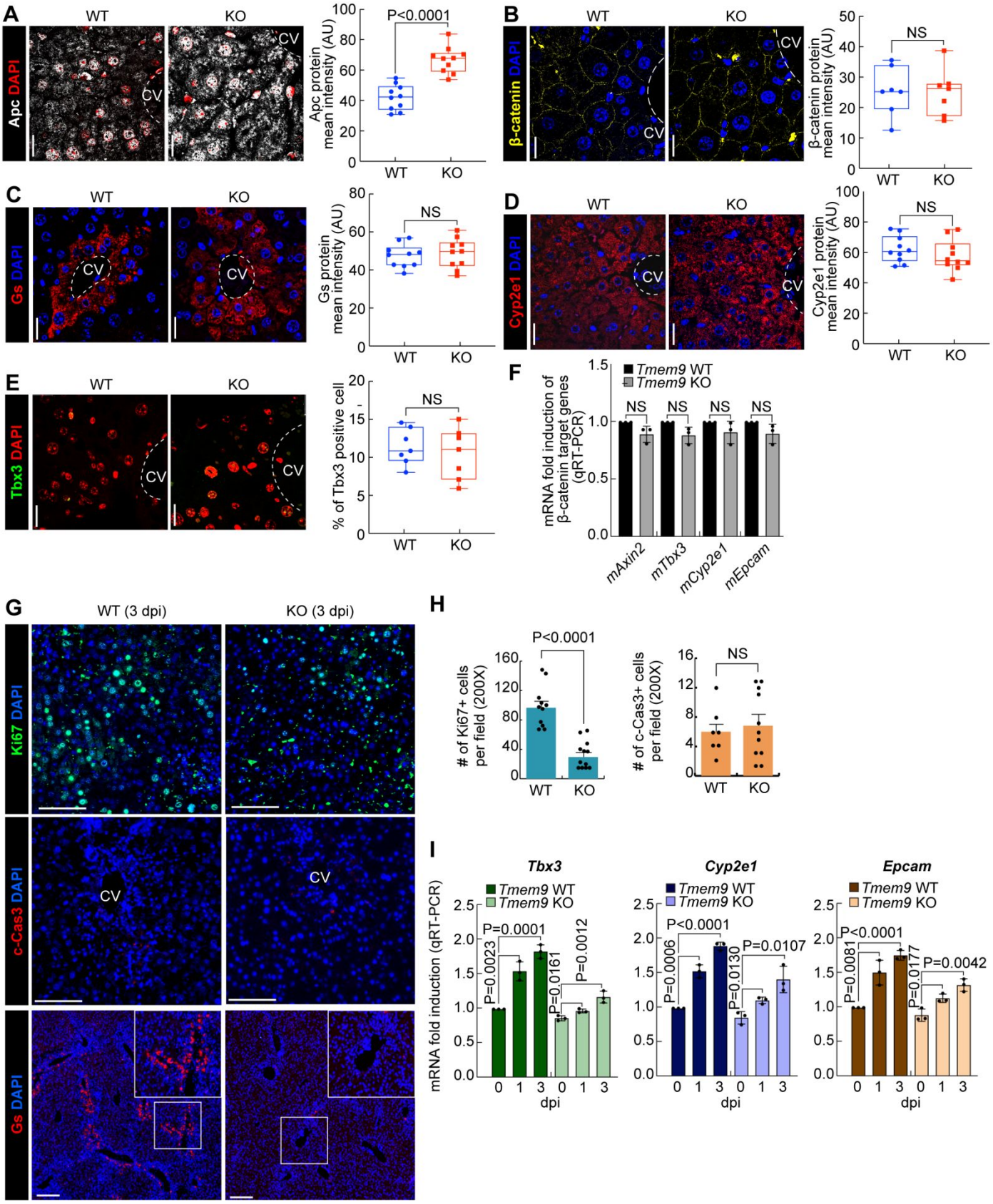

Supplementary Figure S1. Impaired liver regeneration by *Tmem9* knockout (related to Figure 2)

(A-F) No alteration in hepatic homeostasis by *Tmem9* KO. Uninjured *Tmem9* WT and KO mice (4mo) were examined to assess Wnt/β-catenin signaling activity and hepatocyte marker expression. IHC for Apc (A), β-catenin (B), Gs (C), Cyp2e1 (D), and Tbx3 (E). Mean intensity was quantified by ZEN software (Zeiss). qRT-PCR for β-catenin target genes using uninjured *Tmem9* WT and KO liver tissues (F). *S18* gene expression served as an internal control for normalization. NS: Not significant (P>0.05). Scale bars=20μm.

(G and H) Cell proliferation was lower in *Tmem9* KO than in *Tmem9* WT mouse liver tissue upon hepatic injury (CCl_4). Staining of proliferating (Ki67) and apoptotic (cleaved caspase-3 [c-Cas3]) cells (G). Quantification of Ki67+ and c-Cas3+ cells (H). Hepatocyte expansion is downregulated in *Tmem9* KO mice upon hepatic injury. IHC for pericentral hepatocytes (Gs; G). Scale bars=100μm.

(I) The reduced expression of *Tbx3*, *Cyp2e1*, and *Epcam* by *Tmem9* KO in the regenerating liver tissues; qRT-PCR analyses.

Supplementary Figure 2 (related to Figure 3)

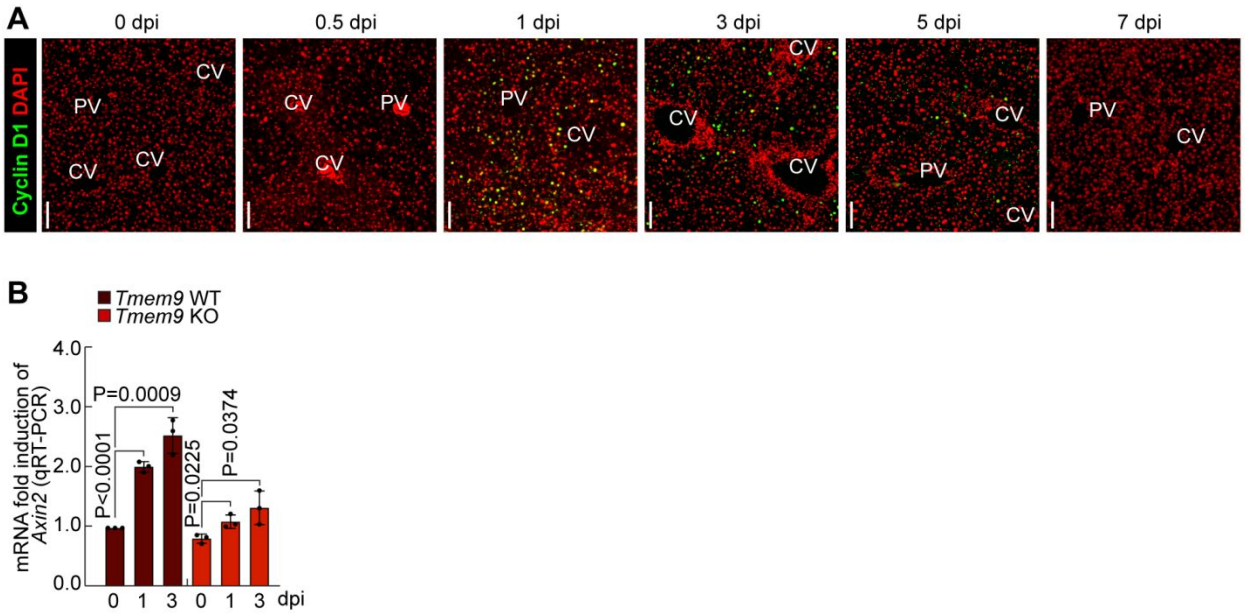

Supplementary Figure S2. TMEM9-activated Wnt/β-catenin signaling during liver regeneration (related to Figure 3)

(A and B) Wnt/β-catenin signaling is activated during liver regeneration. IHC for Cyclin D1 in normal liver tissue after CCl_4 (A). The reduced induction of *Axin2* by *Tmem9* KO in the regenerating liver tissues; qRT-PCR analyses (B). Scale bars=100μm.

Supplementary Figure 3 (related to Figure 3)

A

	Tmem9 WT (n=3)		*Tmem9* KO (n=4)	
	PH	Post-PH (3 days)	PH	Post-PH (3 days)
Body mass (g)	31.71±0.96	30.96±0.92	28.09±1.10	27.36±0.99
Resected liver mass (g)	0.63±0.04	-	0.62±0.09	-
% of body mass	1.98±0.10	-	2.18±0.23	-
Regenerated liver mass (g)	-	0.13±0.02	-	0.11±0.03
% of body mass	-	0.41±0.07	-	0.37±0.11

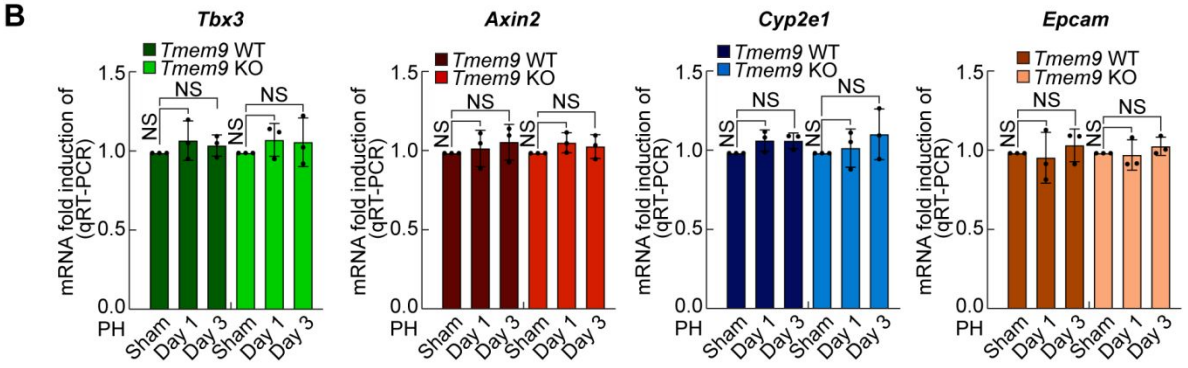

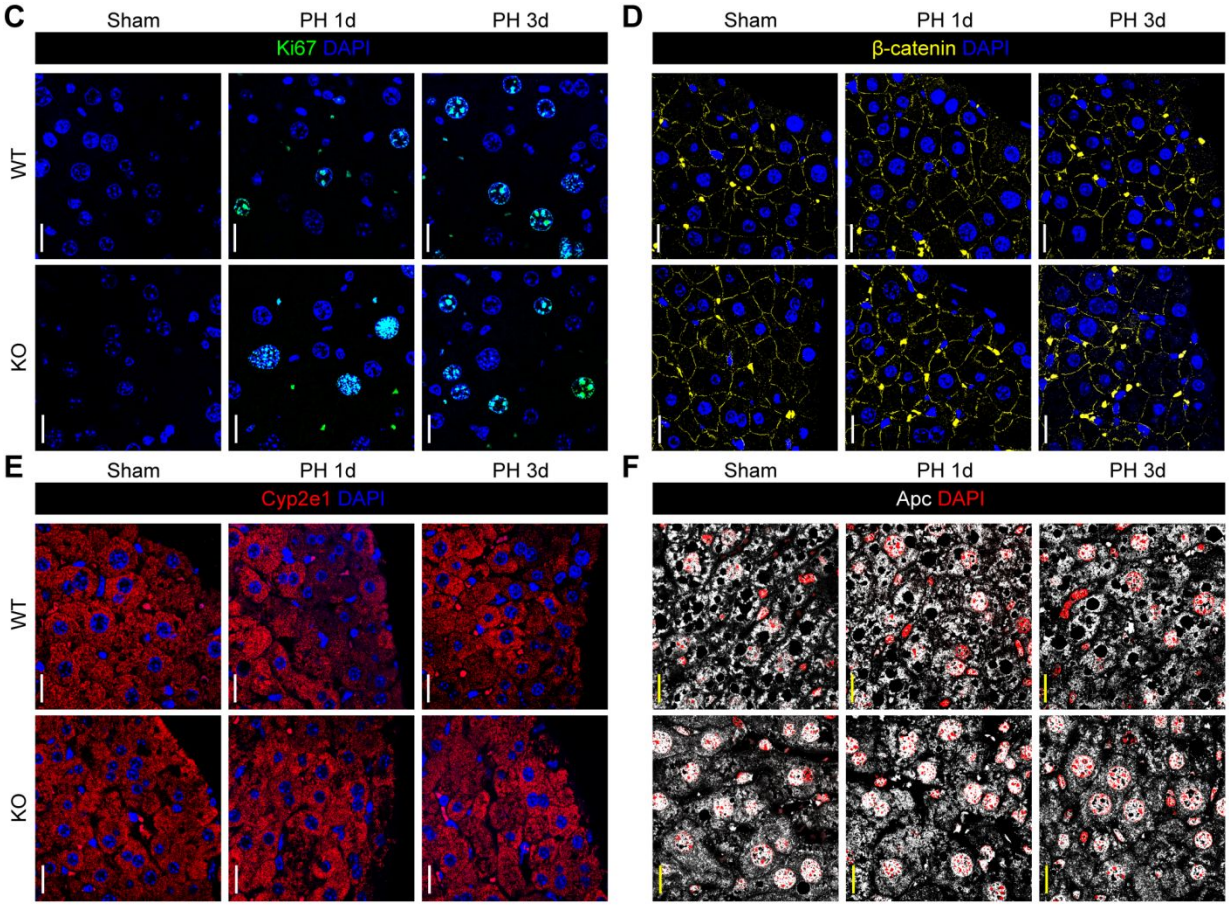

Supplementary Figure S3. No effect of *Tmem9* KO on PH-induced liver regeneration (related to Figure 3)

(A) Quantification of liver regeneration after partial hepatectomy (PH). After 3days PH, mice were sacrificed at 1 or 3 days after surgery and remnant liver tissue was collected for RNA isolation, protein extraction, IHC, and mass quantification.

(B-F) No difference in cell proliferation and Wnt/β-catenin signaling activity by *Tmem9* KO in PH-induced regenerating liver samples. qRT-PCR for β-catenin target genes (B). IHC for Ki67 (C), β-catenin (D), Cyp2e1 (E), and Apc (F). Scale bars=20μm.

Supplementary Figure 4 (related to Figure 4)

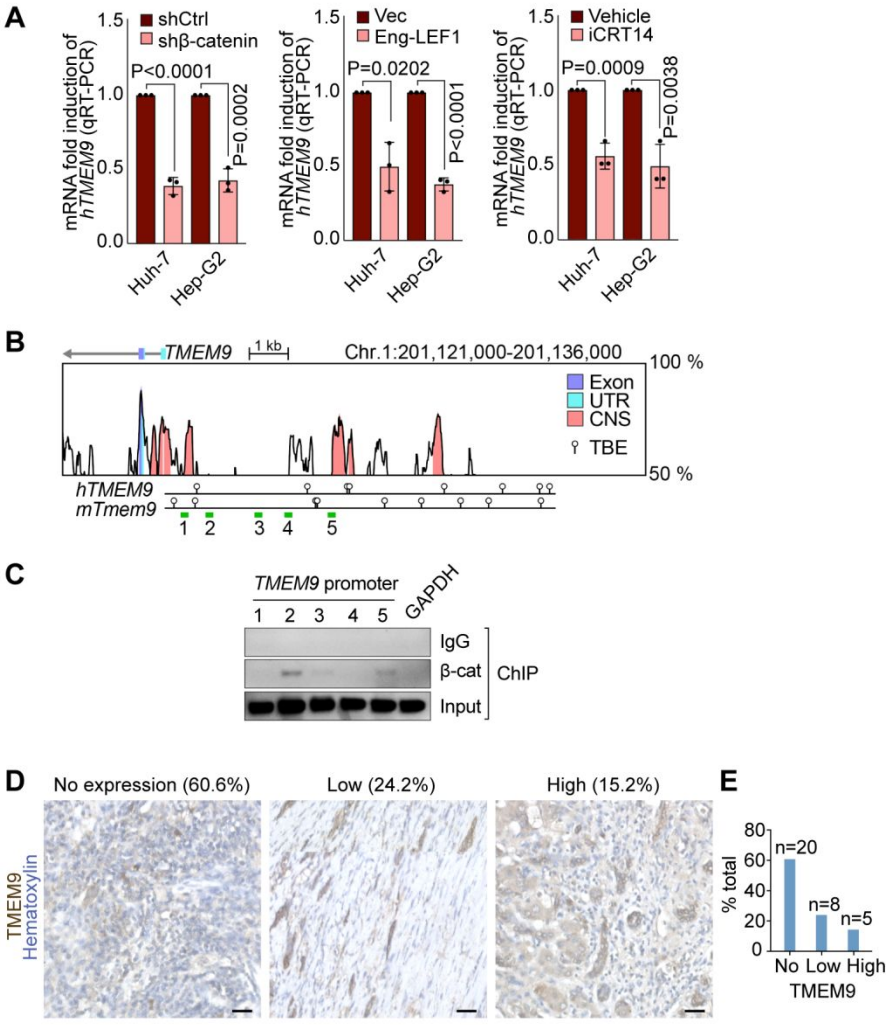

Supplementary Figure S4. Expression of TMEM9 in HCC and liver cirrhosis (related to Figure 4)

(A) Decreased *TMEM9* by β-catenin inhibition. *TMEM9* transcription was downregulated by inhibition of β-catenin with shβ-catenin, Eng-LEF1, or iCRT14 (50μM for 12hr).

(B and C) Transactivation of TMEM9 by β-catenin. Conserved non-coding sequence analysis (B). VISTA genome browser analysis showing conserved non-coding sequence between human and mouse *TMEM9* promoter (1). Chromatin immunoprecipitation (ChIP) analysis of *TMEM9* promoter in HepG2 cells. Five ChIP amplicons were analyzed by ChIP-PCR of β-catenin chromatin immunoprecipitates. ChIP amplicon #2 showed the occupancy by β-catenin.

(D and E) Expression of TMEM9 in liver cirrhosis. Tissue microarray samples (Biomax, Inc., Cat No. LV1401) were immunostained with anti-TMEM9 antibody (D). Thirty-three samples

(normal tissues with cirrhosis; adjacent to cancer) were analyzed for the expression of TMEM9 (no, low, and high)(E). Hematoxylin for nuclear counterstaining; Scale bars=100μm.

Supplementary Figure 5 (related to Figure 5)

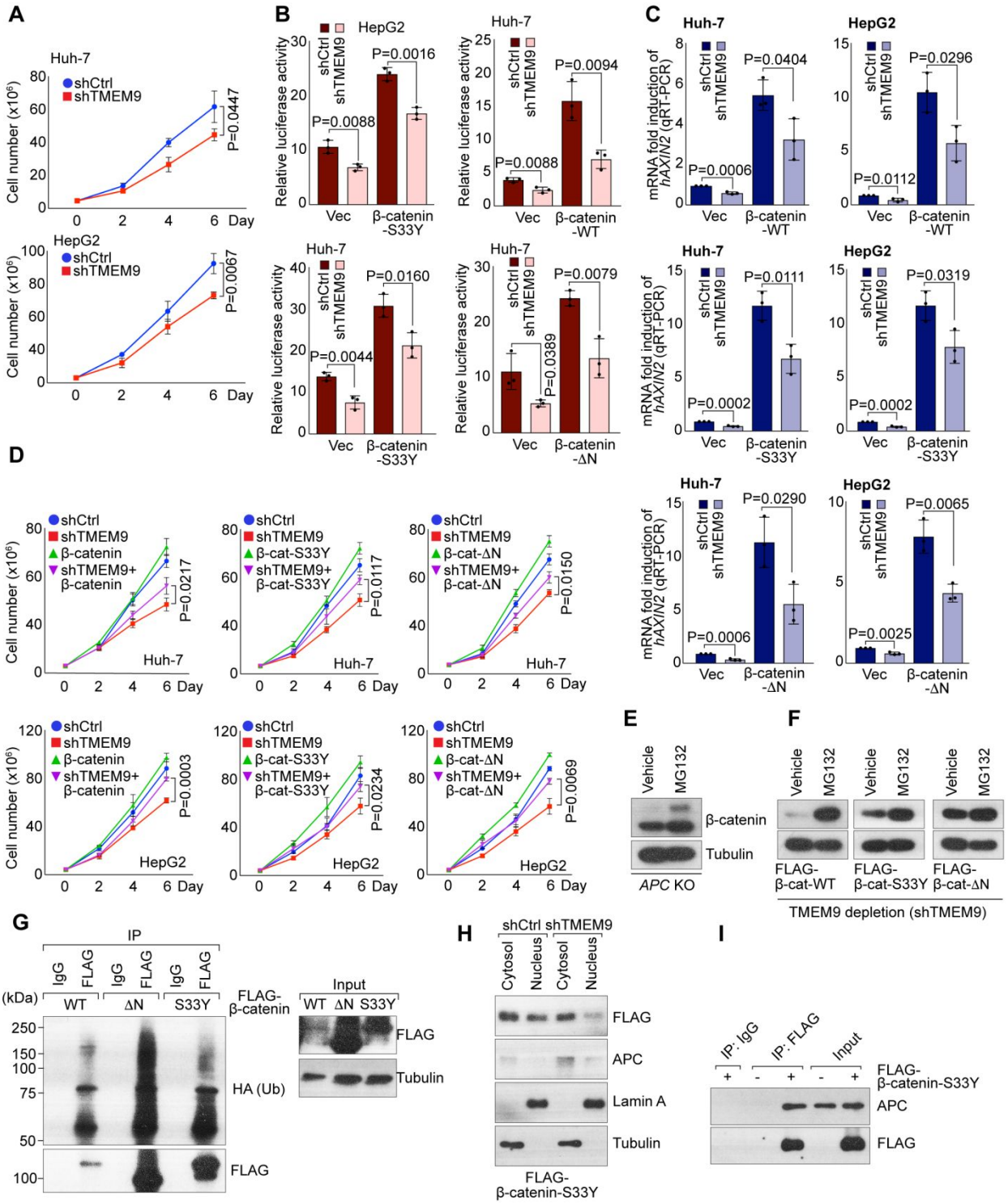

Supplementary Figure S5. Nuclear translocation of β-catenin by TMEM9-downregulated APC (related to Figure 5)

(A) Decreased HCC cell proliferation by TMEM9 depletion. Huh-7 and HepG2 (shCtrl [shGFP] vs. shTMEM9) cell proliferation was analyzed by cell counting.

(B and C) Reduced WT and MT β-catenin transcriptional activity by shTMEM9. Huh-7 and HepG2 cells were transfected with WT or MT (S33Y and ΔN) β-catenin plasmid. Luciferase (TOP/FOPFLASH; B) and qRT-PCR of *AXIN2* (C) were measured to determine β-catenin transcriptional activity.

(D) Downregulation of β-catenin-induced HCC cell proliferation by shTMEM9. Huh-7 and HepG2 (shCtrl and shTMEM9) cells were stably transduced WT or MT β-catenin and analyzed by cell counting.

(E and F) Upregulation of WT and MT β-catenin by proteasome inhibitor. Increased endogenous WT and MT β-catenin by MG132 treatment in HepG2. 6 hours after treatment of vehicle or MG132 (1μM), cells were collected for IB (E). Each indicated β-catenin plasmid was transiently transfected into 293T cells. 24 hours after transfection, cells were treated with MG132 for 6hr (F). Then, 24 hours after treatment, cells were harvested for IB.

(G) Ubiquitination of WT and MT β-catenin. 24 hours after transfection of the indicated plasmids with HA-Ubc, cells were collected for co-IP assay.

(H) Decreased nuclear translocation of MT β-catenin by TMEM9 depletion. After 24hr transfection with S33Y β-catenin plasmid, HepG2 cells were fractionated into the cytosolic and nucleus fractions, followed by IB.

(I) Interaction between APC and S33Y β-catenin. Co-IP analysis.

Supplementary Figure 6 (related to Figure 6)

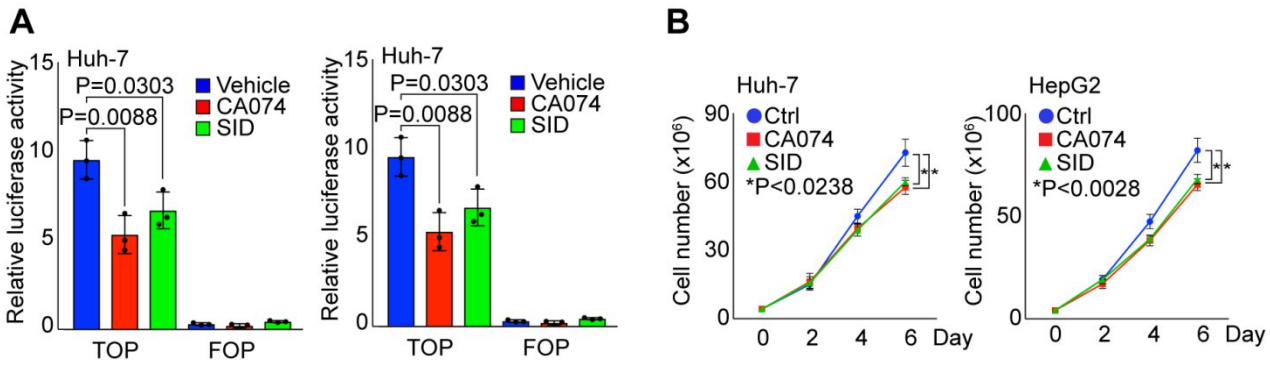

Supplementary Figure S6. Decreased Wnt/β-catenin signaling by lysosomal protease inhibitors (related to Figure 6)

(A) Decreased β-catenin transcriptional activity by lysosomal protease inhibitors. Luciferase (TOP/FOPFLASH) was measured to determine β-catenin transcriptional activity.

(B) Downregulation of HCC cell proliferation by lysosomal protease inhibitors. Huh-7 and HepG2 cell proliferation was analyzed by cell counting.

Supplementary Figure 7 (related to Figure 7)

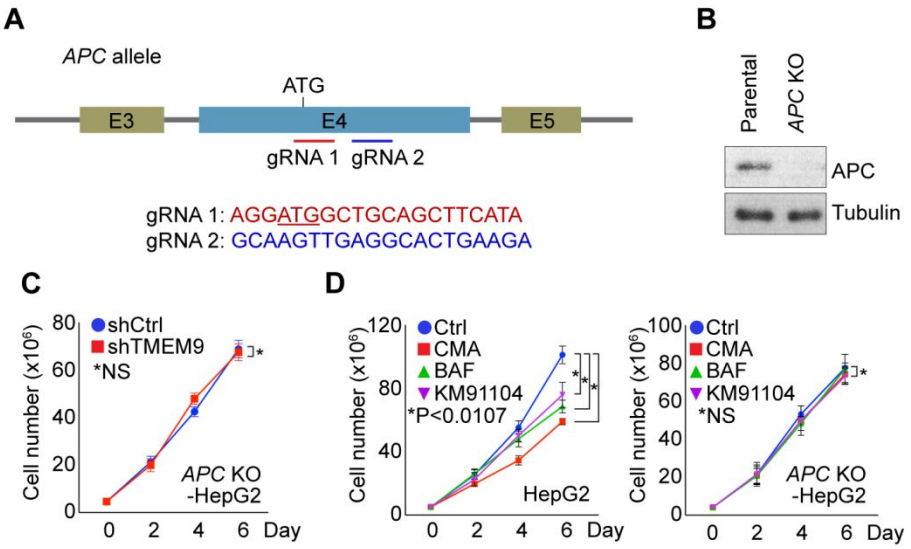

Supplementary Figure S7. Inhibition of HCC cell proliferation by blockade of TMEM9-v-ATPase axis (related to Figure 7)

(A and B) CRISPR/Cas9-mediated targeting of *APC* alleles. The exon 4 of *APC* gene was targeted using two gRNAs for the deletion of the start codon or partial sequence of Exon 4 (A). HepG2 cells were stably transduced with lentivirus encoding Cas9 and gRNAs. Validation of *APC* KO using IB (B).

(C and D) Decreased HCC cell proliferation by TMEM9 depletion and v-ATPase inhibitors. The proliferation of HepG2 cells transfected with shCtrl or shTMEM9 was analyzed by cell counting (C). HepG2 and *APC* KO-HepG2 cells were treated with v-ATPase inhibitors and cells were counted at the indicated time point (D).

Supplementary Table

Supplementary Table 1. Analysis of mutual exclusivity between TMEM9 and Wnt/β-catenin

To identify mutual or exclusive expression between TMEM9 and Wnt/β-catenin related genes in HCC, we used cBioportal (https://www.cbioportal.org) datasets (TCGA, Provision; TCGA PanCancer Atlas).

Supplementary Table 2. Quantitative analysis of TMEM9 expression in normal liver and HCC samples

To determine TMEM9 protein expression, we analyzed 42 normal liver tissue samples (Biomax; LVN801 normal liver) and 64 HCC (Biomax; LV1401 HCC) using IHC for TMEM9. While HCC samples show the high of TMEM9 expression, normal tissue samples display the low or absence of TMEM9 expression.

Supplementary Table 3. Antibody information

Supplementary Table 4. Primer information

Supplementary Experimental Procedures

Constructs

All gene expression plasmids were constructed from cDNA library or open reading frame sources using PCR and cloned into FLAG-pcDNA, FLAG-dTomato-pcDNA, FLAG-pLenti, or FLAG-dTomato-pLenti mammalian expression plasmids. Mutant constructs were generated by site-directed mutagenesis using PCR.

Tmem9 knockout mouse animal model

As previous our study, *Tmem9* KO mouse was established (1). All animal procedures were performed based on the guidelines by Association for the Assessment and Accreditation of Laboratory Animal Care (AAALAC), and the Institutional (MD Anderson Cancer Center) approved protocols (IACUC00001141; University of Texas MD Anderson Cancer Center Institutional Animal Care and Use Committee). The study is compliant with all relevant ethical regulations regarding animal research.

Mammalian cell culture

Cell lines (Huh-7, HepG2, and HEK293T) were purchased from American Type Culture Collection and maintained in Dulbecco's modified Eagle medium (containing 10% fetal bovine serum and 1% Penicillin-Streptomycin). Mycoplasma screening was performed using MycoAlert™ Mycoplasma Detection Kit (Lonza). Lentiviral plasmids encoding shRNAs were purchased from Open Biosystems. To establish cell lines stably expressing shRNAs or genes, each cell line was transduced with lentiviruses, and selected by puromycin (1-2μg/ml) for two days. The following reagents were also used: CCl_4 (Sigma), bafilomycin A1 (Wako), concanamycin A (Sigma), KM91104 (Millipore), CA074 (R&D systems), and SID26681509 (R&D systems).

Reporter assays

The reporter plasmids, pMegaTOPFLASH and pMegaFOPFLASH (2, 3), were transiently transfected with pSV40-Renilla plasmid (internal control) and analyzed using Dual Luciferase assay system (Promega).

Immunofluorescence staining and immunohistochemistry

Using PEI, cells were transiently transfected with plasmids. Cells grown on glass coverslips were washed and fixed in 4% paraformaldehyde for 10min at 4°C. After blocking with 5% goat serum in PBS for 30min, antibodies were treated for immunostaining cells. Liver samples were fixed in 10% neutral buffered formalin overnight and embedded in paraffin. Tissue samples were then sectioned (5μm) and H&E staining was performed following standard procedure. For IHC, slides were deparaffinized, rehydrated, processed for antigen retrieval, blocked, incubated with primary antibody, and fluorescence-conjugated secondary antibody. Next, slides were mounted with DAPI (Invitrogen), sealed, and photographed using an inverted microscope (Zeiss; AxioVision). For comparison among the experiment groups, images were captured with the same exposure time. The detailed information regarding antibodies can be found in Supplementary Table 3.

Gene expression analysis

RNAs were extracted by TRIzol (Invitrogen) and converted to cDNAs using iScript cDNA

synthesis kit (Biorad) with 1µg of RNA. For gene expression analysis, semiquantitative RT-PCR or qRT-PCR was performed. qRT PCR results were quantified by comparative $2^{-\Delta\Delta Ct}$ methods (Applied Biosystems). For internal controls, *HPRT1* was used. The primer sequences can be found in Supplementary Table 4.

APC somatic cell targeting

The *APC* KO cells were established using the clustered regularly interspaced short palindromic repeat (CRISPR) using a lentiviral CRISPR v2 vector (Addgene). The lentiviral plasmid contains two expression cassettes, hSpCas9 and the chimeric guide RNA (gRNA) where oligos were cloned, based on the protospacer adjacent motif (PAM) on the target site. The lentiCRISPRv2 plasmids were transfected into HEK293T cells along with pCMV-ΔR8.2 dVPR and pCMV-VSVG plasmids for lentiviral packaging. HCC cell lines were then transduced with lentiviruses and selected in puromycin for 72hr. After selection, three clonally selected cell lines were used for analysis. *APC* KO was confirmed by IB. *APC* gRNA sequences: #1: 5'-AGGATGGCTGCAGCTTCATA -3'; #2: 5'- GCAAGTTGAGGCACTGAAGA -3'.

Immunoblotting and immunoprecipitation

Whole-cell lysates of mammalian cells were prepared using NP-40 lysis buffer (0.5% NP-40, 1.5mM MgCl2, 25mM HEPES, 150mM KCl, 10% glycerol, 1mM phenylmethylsulfonyl fluoride, 12.7mM benzamidine HCl, 0.2mM aprotinin, 0.5mM leupeptin and 0.1mM pepstatin A) for 20min at 4°C followed by centrifugation (14,000rpm for 10min). Supernatants were denatured in 5xSDS sample buffer (200mM Tris-HCl pH6.8, 40% glycerol, 8% SDS, 200mM dithiothreitol and 0.08% bromophenol blue) at 95°C for 5min followed by SDS–PAGE. For immunoblot blocking and antibody incubation, 0.1% non-fat dry milk in Tris-buffered saline and Tween-20 (25mM Tris-HCl pH8.0, 125mM NaCl and 0.5% Tween-20) was used. SuperSignal West Pico (Thermo; 34087) and Femto (Thermo; 34095) reagents were used to detect horseradish peroxidase-conjugated secondary antibodies. For immunoprecipitation, cell lysates were incubated with 20µl of magnetic beads (Sigma; M8823) for 2hr. Immunoprecipitates were then washed with cell lysis buffer 3 times, eluted using an SDS sample buffer, and analyzed using immunoblotting. The detailed information regarding antibodies can be found in Supplementary Table 3.

Duolink assays

For the visualization of protein interaction *in situ*, cells were seeded onto the cover glass. After fixation with 4% paraformaldehyde for 5min, cells were permeabilized with 0.01% Triton-x100 for Duolink assays, as manufacturer's (Sigma; DUO92101) recommended protocol: blocking, primary antibody reaction, (+) and (-) probe reaction, ligation, polymerization, and amplification.

Acute CCl_4 injury mouse model

Male mice (older than eight weeks) were injected with carbon tetrachloride (CCl4; Sigma) for acute liver injury model. CCl4 was dissolved in corn oil (Fisher) at a final concentration of 20% (v/v) for intraperitoneal administration (1 ml/kg). Mice were sacrificed at various time points, and liver tissues were collected for further analyses.

Partial hepatectomy (PH)

PH (70% removal of the total liver) or sham control surgery was performed with isoflurane anesthesia. Three to four WT C57BL/B6 and *Tmem9* KO (6 months of age)

mice were used for PH according to guidelines of the institutional Animal Care and Use Committee of the University of Texas, MD Anderson Cancer Center. Mice were sacrificed at 1 or 3 days after surgery and remnant liver tissue was collected. Flash-frozen liver tissues were processed for RNA isolation, protein extraction, IHC, and mass.

Xenograft assays

Mice (BALB/c nude) were subcutaneously injected with 5 x 10^6 cells of HepG2 cells (shCtrl vs. shTMEM9; shTMEM9-Vec vs. shTMEM-β-catenin; Ctrl vs. BAF [*APC* WT and KO]). After 3 weeks for adaptation, tumors were collected for assessment of tumor weight, RNA, IB, and IHC.

Fluorescence recovery after photobleaching (FRAP) assay

HepG2 cells were grown on chambered coverglass (Nunc) and were transfected with dTomato-β-catenin (WT and ΔN). After 24hr transfection in 5% CO_2 at 37℃, images were acquired by using a LSM880-Airyscan confocal (Zeiss). For photobleaching experiments, samples were photobleached with a solid-state laser using LSM880-Airyscan confocal. Nucleus was bleached for 1000s at 100% laser power. The samples were imaged every 5s for 60s with a separate 555nm laser. The average fluorescence mean intensities of nucleus were measured using Zen software (Zeiss). The recovery curves shown are the averages of at least 8 cells from at least three independent experiments.

In silico analysis of TMEM9 expression and genetic alteration

TMEM9 expression in HCC cells was analyzed in the cBioportal (www.cbioportal.org), and PICB database (www.Picb.ac.cn/PDXliver). The cBioportal analysis was performed with default options using TCGA (provisional and PanCancer) and AMC data sets for gene alterations (mutations and copy number change).

Chromatin immunoprecipitation assay (ChIP)

Cells were crosslinked with 1% formaldehyde for 15 min at room temperature, and quenched by glycine (0.125 M). After washing with cold PBS, tissues were incubated with lysis buffer (0.5% NP-40, 25mM HEPES, 150mM KCl, 1.5mM $MgCl_2$, 10% glycerol and KOH pH 7.5) containing protease inhibitor for 15 min on ice. Cell lysates were centrifuged (1,677g for 5min), and supernatants were discarded. Cell pellets were subjected to sonication with nuclear lysis buffer (50mM Tris pH8.0, 10mM EDTA, 1% SDS), using Bioruptor Plus sonication device (Diagnode). Supernatant were diluted 20 times in IP buffer (50mM Tris pH8.0, 150mM NaCl, 0.5% NP- 40, protease inhibitor mixtures) and subjected to IP with antibody against β-catenin or normal rabbit IgG. Immunoprecipitates were also washed serially with ChIP-RIPA lysis buffer, high salt (50mM Tris, pH8.0; 500mM NaCl; 0.1% SDS, 0.5% deoxycholate, 1% NP-40 and 1mM EDTA), LiCl wash buffer (50mM Tris, pH8.0; 1 mM EDTA, 250mM LiCl; 1% NP-40 and 0.5% deoxycholate) and Tris-EDTA buffer. Finally, immunoprecipitate crosslinking was reversed by incubation at 65 °C overnight and treated with RNase A and proteinase K to extract DNA. The ChIP PCR primer sequences of TMEM9 promoters amplicons was described in a previous paper. GAPDH promoter amplicons served as negative control.

Cell proliferation assays

Using plasmids stably expressing cells, the number of cells was counted using hematocytometer as an indicated growth days.

Statistics and reproducibility

The Student's t-test was used for comparisons of two groups (n≥3). P values less than 0.05 were considered significant. Error bars indicate standard deviation, which indicates standard error of the mean. All experiments were performed three or more times with similar results, independently under identical or similar conditions.

Antibody information

See Supplementary Table 3 for a complete list of antibodies.

Primer information

See Supplementary Table 4 for a complete list of primers.

Supplementary References

1. Jung YS, Jun S, Kim MJ, Lee SH, Suh HN, Lien EM, Jung HY, et al. TMEM9 promotes intestinal tumorigenesis through vacuolar-ATPase-activated Wnt/beta-catenin signalling. Nat Cell Biol 2018;20:1421-1433.
2. Hu M, Kurobe M, Jeong YJ, Fuerer C, Ghole S, Nusse R, Sylvester KG. Wnt/beta-catenin signaling in murine hepatic transit amplifying progenitor cells. Gastroenterology 2007;133:1579-1591.
3. Park JI, Venteicher AS, Hong JY, Choi J, Jun S, Shkreli M, Chang W, et al. Telomerase modulates Wnt signalling by association with target gene chromatin. Nature 2009;460:66-72.

Table S1. Analysis of mutual exclusivity between TMEM9 and Wnt/beta-catenin signaling

Liver Hepatocellular Carcinoma (TCGA, Provisional)								
360 samples								
Gene A	Gene B	Neither	A Not B	B Not A	Both	Log Odds Ratio	p-Value	Tendency
CTNNB1	AXIN2	244	71	16	29	1.829	<0.001	Co-occurrence
CTNNB1	AXIN1	206	94	54	6	-1.413	<0.001	Mutual exclusivity
CTNNB1	TMEM9	168	78	92	22	-0.663	0.009	Mutual exclusivity
APC	AXIN1	269	31	59	1	-1.917	0.018	Mutual exclusivity
APC	AXIN2	290	25	38	7	0.759	0.087	Co-occurrence
AXIN1	TMEM9	209	37	91	23	0.356	0.144	Co-occurrence
AXIN1	AXIN2	260	55	40	5	-0.526	0.199	Mutual exclusivity
APC	TMEM9	222	24	106	8	-0.359	0.262	Mutual exclusivity
AXIN2	TMEM9	213	33	102	12	-0.275	0.278	Mutual exclusivity
APC	CTNNB1	236	24	92	8	-0.157	0.446	Mutual exclusivity
Liver Hepatocellular Carcinoma (TCGA, PanCancer Atlas)								
348 samples								
Gene A	Gene B	Neither	A Not B	B Not A	Both	Log Odds Ratio	p-Value	Tendency
AXIN2	RNF43	295	17	14	22	>3	<0.001	Co-occurrence
CTNNB1	RNF43	241	71	9	27	2.321	<0.001	Co-occurrence
CTNNB1	AXIN2	239	70	11	28	2.162	<0.001	Co-occurrence
CTNNB1	AXIN1	197	92	53	6	-1.417	<0.001	Mutual exclusivity
APC	AXIN1	261	28	58	1	-1.828	0.027	Mutual exclusivity
TMEM9	RNF43	218	94	31	5	-0.983	0.027	Mutual exclusivity
CTNNB1	TMEM9	172	77	78	21	-0.508	0.044	Mutual exclusivity
APC	AXIN2	286	23	33	6	0.816	0.09	Co-occurrence

AXIN1	RNF43	256	56	33	3	-0.878	0.106	Mutual exclusivity
AXIN2	TMEM9	218	31	91	8	-0.481	0.164	Mutual exclusivity
APC	RNF43	288	24	31	5	0.66	0.167	Co-occurrence
AXIN1	AXIN2	254	55	35	4	-0.639	0.17	Mutual exclusivity
APC	TMEM9	226	23	93	6	-0.456	0.23	Mutual exclusivity
AXIN1	TMEM9	209	40	80	19	0.216	0.29	Co-occurrence
APC	CTNNB1	228	22	91	7	-0.227	0.397	Mutual exclusivity

Supplementary Table 2. Quantitative analysis of TMEM9 expression in normal liver and HCC samples

No.	TMEM9	Age	Sex	Organ	Pathology diagnosis	TNM	Grade	Stage	Type	Tissue ID.
1	N	2	F	Liver	Normal liver tissue	-	-	-	normal	DIv03N002
2	L	2	F	Liver	Normal liver tissue	-	-	-	normal	DIv03N002
3	N	56	M	Liver	Normal liver tissue	-	-	-	normal	DIv03N003
4	N	56	M	Liver	Normal liver tissue	-	-	-	normal	DIv03N003
5	L	50	F	Liver	Normal liver tissue	-	-	-	normal	DIv03N005
6	L	50	F	Liver	Normal liver tissue	-	-	-	normal	DIv03N005
7	N	35	F	Liver	Normal liver tissue	-	-	-	normal	DIv03N009
8	N	35	F	Liver	Normal liver tissue	-	-	-	normal	DIv03N009
9	L	21	F	Liver	Normal liver tissue	-	-	-	normal	DIv05N001
10	N	21	F	Liver	Normal liver tissue	-	-	-	normal	DIv05N001
11	L	35	M	Liver	Normal liver tissue	-	-	-	normal	DIv05N006
12	L	35	M	Liver	Normal liver tissue	-	-	-	normal	DIv05N006
13	N	35	M	Liver	Normal liver tissue	-	-	-	normal	DIv05N010
14	N	35	M	Liver	Normal liver tissue	-	-	-	normal	DIv05N010
15	L	45	M	Liver	Normal liver tissue	-	-	-	normal	DIv06N001
16	L	45	M	Liver	Normal liver tissue	-	-	-	normal	DIv06N001
17	L	47	M	Liver	Normal liver tissue	-	-	-	normal	DIv06N004
18	L	47	M	Liver	Normal liver tissue	-	-	-	normal	DIv06N004
19	H	16	M	Liver	Normal liver tissue	-	-	-	normal	DIv06N007
20	L	16	M	Liver	Normal liver tissue	-	-	-	normal	DIv06N007
21	N	18	F	Liver	Normal liver tissue	-	-	-	normal	DIv06N010
22	N	18	F	Liver	Normal liver tissue	-	-	-	normal	DIv06N010
23	L	43	M	Liver	Normal liver tissue	-	-	-	normal	DIv06N019
24	N	43	M	Liver	Normal liver tissue	-	-	-	normal	DIv06N019
25	L	3	M	Liver	Normal liver tissue	-	-	-	normal	DIv06N026
26	L	3	M	Liver	Normal liver tissue	-	-	-	normal	DIv06N026
27	L	47	M	Liver	Normal liver tissue	-	-	-	normal	DIv06N028
28	L	47	M	Liver	Normal liver tissue	-	-	-	normal	DIv06N028
29	L	21	F	Liver	Normal liver tissue	-	-	-	normal	DIv06N023
30	L	21	F	Liver	Normal liver tissue	-	-	-	normal	DIv06N023
31	N	40	F	Liver	Normal liver tissue	-	-	-	normal	DIv07N002
32	L	40	F	Liver	Normal liver tissue	-	-	-	normal	DIv07N002
33	L	21	F	Liver	Normal liver tissue	-	-	-	normal	DIv07N018
34	N	21	F	Liver	Normal liver tissue	-	-	-	normal	DIv07N018
35	L	3	M	Liver	Normal liver tissue	-	-	-	normal	DIv07N021
36	L	3	M	Liver	Normal liver tissue	-	-	-	normal	DIv07N021
37	L	36	M	Liver	Normal liver tissue	-	-	-	normal	DIv08N032
38	L	36	M	Liver	Normal liver tissue	-	-	-	normal	DIv08N032
39	L	2	F	Liver	Normal liver tissue	-	-	-	normal	DIv08N035
40	L	2	F	Liver	Normal liver tissue	-	-	-	normal	DIv08N035
41	N	34	M	Liver	Normal liver tissue	-	-	-	normal	DIv08N042
42	L	34	M	Liver	Normal liver tissue	-	-	-	normal	DIv08N042

No.	TMEM9	Age	Sex	Organ	Pathology diagnosis	TNM	Grade	Stage	Type	Tissue ID.
1	L (low)	35	F	Liver	Hepatocellular carcinoma	T2N0M0	1	II	Malignant	DIv051363
2	H (high)	63	M	Liver	Hepatocellular carcinoma	T3N0M0	2	III	Malignant	DIv031882
3	H (high)	28	M	Liver	Hepatocellular carcinoma	T3N0M0	1	IIIA	Malignant	DIv061996
4	H (high)	51	F	Liver	Hepatocellular carcinoma	T1N0M0	2	I	Malignant	DIv050679
5	H (high)	65	M	Liver	Hepatocellular carcinoma	T2N0M0	2	II	Malignant	DIv024468
6	L	41	M	Liver	Hepatocellular carcinoma	T2N0M0	2	II	Malignant	DIv030296
7	H (high)	67	F	Liver	Hepatocellular carcinoma	T3N0M0	2	III	Malignant	DIv010744
8	H (high)	55	M	Liver	Hepatocellular carcinoma	T4N0M0	2	IVA	Malignant	DIv051677
9	H (high)	49	M	Liver	Hepatocellular carcinoma	T3N0M0	1	IIIA	Malignant	DIv080272
10	H (high)	63	M	Liver	Hepatocellular carcinoma	T3N0M0	3	III	Malignant	DIv030341
11	H (high)	58	F	Liver	Hepatocellular carcinoma	T1N0M0	1	I	Malignant	DIv140256
12	H (high)	62	M	Liver	Hepatocellular carcinoma	T3N0M0	1	III	Malignant	DIv011241
13	H (high)	58	M	Liver	Hepatocellular carcinoma	T3N0M0	1	IIIA	Malignant	DIv051446
14	L	64	M	Liver	Hepatocellular carcinoma	T3N1M0	2	IVA	Malignant	DIv062329
15	B+N	56	M	Liver	Hepatocellular carcinoma	T2N0M0	2	II	Malignant	DIv070039
16	L	60	M	Liver	Hepatocellular carcinoma	T3N0M0	2	IIIA	Malignant	DIv062244
17	H (high)	56	M	Liver	Hepatocellular carcinoma	T3N0M0	2	IIIA	Malignant	DIv061934
18	H (high)	55	M	Liver	Hepatocellular carcinoma	T4N0M0	2	IIIC	Malignant	DIv051669
19	H (high)	67	M	Liver	Hepatocellular carcinoma	T2N0M0	2	II	Malignant	DIv041729
20	H (high)	41	M	Liver	Hepatocellular carcinoma	T3N0M0	2	III	Malignant	DIv040276
21	B+N	48	M	Liver	Hepatocellular carcinoma	T2N0M0	2	II	Malignant	DIv060204
22	H (high)	66	M	Liver	Hepatocellular carcinoma	T2N0M0	2	II	Malignant	DIv050594
23	H (high)	50	M	Liver	Hepatocellular carcinoma	T2N0M0	2	II	Malignant	DIv031874
24	H (high)	43	M	Liver	Hepatocellular carcinoma	T3N0M0	-	IIIA	Malignant	DIv030116
25	H (high)	63	M	Liver	Hepatocellular carcinoma	T3N0M0	3	IIIA	Malignant	DIv010376
26	L	50	M	Liver	Hepatocellular carcinoma	T3N0M0	2	III	Malignant	DIv041081
27	H (high)	49	M	Liver	Hepatocellular carcinoma	T2N0M0	2	II	Malignant	DIv040931
28	L	70	M	Liver	Hepatocellular carcinoma	T3N0M0	1	IIIA	Malignant	DIv030662
29	H (high)	45	M	Liver	Hepatocellular carcinoma	T3N0M0	2	IIIA	Malignant	DIv062119
30	H (high)	53	M	Liver	Hepatocellular carcinoma	T2N0M0	2	II	Malignant	DIv022896
31	H (high)	66	M	Liver	Hepatocellular carcinoma	T3N0M0	2	IIIA	Malignant	DIv050491
32	M	60	M	Liver	Hepatocellular carcinoma with necrosis	T2N0M0	2	II	Malignant	DIv062758
33	L	60	M	Liver	Hepatocellular carcinoma	T2N0M0	2	II	Malignant	DIv024197
34	H (high)	34	M	Liver	Hepatocellular carcinoma	T2N0M0	2	II	Malignant	DIv041727
35	M	48	M	Liver	Hepatocellular carcinoma	T3N0M0	2	IIIA	Malignant	DIv010243
36	H (high)	55	M	Liver	Hepatocellular carcinoma	T2N0M0	2	II	Malignant	DIv051889
37	H (high)	57	M	Liver	Hepatocellular carcinoma	T4N1M1	2	IVB	Malignant	DIv062615
38	H (high)	35	M	Liver	Hepatocellular carcinoma	T3N0M0	2	IIIA	Malignant	DIv010984
39	H (high)	48	M	Liver	Hepatocellular carcinoma	T2N0M0	2	II	Malignant	DIv060204
40	L	47	M	Liver	Hepatocellular carcinoma	T3N0M0	2	IIIA	Malignant	DIv030194
41	H (high)	52	F	Liver	Hepatocellular carcinoma	T3N0M0	2	IIIA	Malignant	DIv010201
42	N	38	M	Liver	Hepatocellular carcinoma	T2N0M0	2	II	Malignant	DIv040977
43	B+N	52	M	Liver	Hepatocellular carcinoma	T3N1M0	-	III	Malignant	DIv062807
44	H (high)	53	M	Liver	Hepatocellular carcinoma	T3N0M0	3	III	Malignant	DIv011246
45	H (high)	43	M	Liver	Hepatocellular carcinoma	T3N0M0	3	III	Malignant	DIv050775
46	H (high)	58	M	Liver	Hepatocellular carcinoma	T3N0M0	3	IIIA	Malignant	DIv030949

47	H (high)	45	M	Liver	Hepatocellular carcinoma	T2N0M0	3	II	Malignant	Dlv030792
48	H (high)	38	M	Liver	Hepatocellular carcinoma	T3N0M0	3	IIIA	Malignant	Dlv060798
49	H (high)	56	F	Liver	Hepatocellular carcinoma	T2N0M0	3	II	Malignant	Dlv040632
50	H (high)	41	F	Liver	Hepatocellular carcinoma	T3N0M0	3	III	Malignant	Dlv041802
51	H (high)	52	M	Liver	Hepatocellular carcinoma	T3N0M0	3	IIIA	Malignant	Dlv010339
52	L	62	M	Liver	Hepatocellular carcinoma with necrosis	T2N0M0	3	II	Malignant	Dlv051222
53	H (high)	32	M	Liver	Hepatocellular carcinoma with necrosis (sparse)	T4N0M0	3	IVA	Malignant	Dlv061948
54	M+N	68	M	Liver	Hepatocellular carcinoma	T2N0M0	3	II	Malignant	Dlv032013
55	H (high)	60	M	Liver	Hepatocellular carcinoma	T3N0M0	-	IIIA	Malignant	Dlv061541
56	L	42	M	Liver	Hepatocellular carcinoma	T2N0M0	3	II	Malignant	Dlv010980
57	H (high)	52	M	Liver	Hepatocellular carcinoma	T3N0M0	3	IIIA	Malignant	Dlv062343
58	H (high)	59	M	Liver	Hepatocellular carcinoma	T3N0M0	3	III	Malignant	Dlv040314
59	H (high)	49	M	Liver	Hepatocellular carcinoma	T3N0M0	3	IIIA	Malignant	Dlv030993
60	B+N (blank, none)	46	M	Liver	Hepatocellular carcinoma with necrosis	T3N0M0	3	IIIA	Malignant	Dlv030003
61	L	61	M	Liver	Hepatocellular carcinoma with necrosis	T3N1M0	3	IVA	Malignant	Dlv062342
62	H (high)	53	M	Liver	Hepatocellular carcinoma	T2N0M0	3	II	Malignant	Dlv040056
63	H (high)	48	F	Liver	Hepatocellular carcinoma	T2N0M0	-	II	Malignant	Dlv130001
64	H (high)	48	F	Liver	Hepatocholangiocarcinoma	T2N0M0	1	II	Malignant	Dlv080343
65	L	60	M	Liver	Hepatocholangiocarcinoma	T3N1M0	1	IIIB	Malignant	Dlv080175
66	H (high)	67	M	Liver	Hepatocholangiocarcinoma	T3N0M0	1	IIIA	Malignant	Dlv051265
67	H (high)	56	F	Liver	Hepatocholangiocarcinoma	T2N0M0	-	II	Malignant	Dlv051883
68	H (high)	58	M	Liver	Hepatocholangiocarcinoma	T2N0M0	2	II	Malignant	Dlv090030
69	H (high)	49	M	Liver	Hepatocholangiocarcinoma	T2N0M0	2	II	Malignant	Dlv120372
70	H (high)	55	F	Liver	Hepatocholangiocarcinoma	T2N1M0	2	IVA	Malignant	Dlv090215
71	L	64	M	Liver	Hepatocholangiocarcinoma	T4N0M0	3	IVA	Malignant	Dlv040512
72	H (high)	57	F	Liver	Hepatocholangiocarcinoma	T2N1M0	2	IVA	Malignant	Dlv090205
73	H (high)	50	M	Liver	Hepatocholangiocarcinoma	T2N0M0	3	II	Malignant	Dlv070164
74	L	63	F	Liver	Hepatocholangiocarcinoma	T2N1M0	3	IVA	Malignant	Dlv080380
75	H (high)	47	F	Liver	Hepatocholangiocarcinoma with necrosis	T2N1M0	3	IVA	Malignant	Dlv090216
79	N	70	F	Liver	Metastatic carcinoma of fibrofatty tissue	-	-	-	Malignant	Dlv040609
80	L	65	M	Liver	Metastatic carcinoma of fibrofatty tissue	-	-	-	Malignant	Dlv040608

Supplementary Table 4. Primer information

hCTGF (for qRT-PCR)	*mTBX3 for qRT-PCR*
F CCG TAC TCC CAA AAT CTC CAA GCC TA	F GAGGAGAGGCATAAGAAGGAGAC
R CCG TCG GTA CAT ACT CCA CAG AAT TT	R CACAGATCTTTGAGGTTGGATGT
hCYR61 (for qRT-PCR)	*hCYP2E1 for qRT-PCR*
F GAT GGG GAG ACA TTT TCC AAG AAC GT	F CAGAACACTTCCTGAATGAAAATG
R TGT AGA AGG GAA ACG CTG CTT CAT TG	R TTCAAATTAAAATGCTGCAAAATG
hHES1 (for qRT-PCR)	*mCyp2e1 for qRT-PCR*
F CCG GAT AAA CCA AAG ACA GCA TCT GA	F TTCGATTACGATGACAAGAAGTGT
R TCA GCT GGC TCA GAC TTT CAT TTA TT	R TGTGGCTTCCAGGTAGATATTGTA
hHEY1 (for qRT-PCR)	*hEpCAM for qRT-PCR*
F AGT ACA GCT CCT CGG ACA GCG AGC TG	F AATTCTCAATGCAGGGTCTAAAAG
R TGG GGA CAT GGA ACC TAG AGC CGA AC	R ATCTCACCCATCTCCTTTATCTCA
hGLI1 (for qRT-PCR)	*mEpcam for qRT-PCR*
F GTG ATA TGT CCA GCC CCA ACT CCA CA	F ATGTTATCACCATTGATCTGATGC
R GAT TCA GGC TCA CGC TTC TCC TCT CT	R ATGCTCTTAGAAGAATGGAACAGG
hPTCH1 (for qRT-PCR)	*hTMEM9 for qRT-PCR*
F ACA TCT ACC TGA CGG CTT GGG TCA GC	F TTATCTTTGGTGGCTGTGGTC
R CTT TGT CGT GGA CCC ATT CTG GTC GG	R CGAGCATCCTCATTCTCCTC
hPTHLH (for qRT-PCR)	*mTmem9 for qRT-PCR*
F CAA GAT TTA CGG CGA CGA TTC TTC CT	F ATTTACAACCAGAATGTGTCTCAGAA
R GAG AGG GCT TGG AGT TAG GGG ACA CC	R GTAGATGACAATAATGACCTTGATGG
hRUNX2 (for qRT-PCR)	*mWnt2 for qRT-PCR*
F GAC GAG GCA AGA GTT TCA CCT TGA CC	F GAGGTTTAAGAAGCCAACGAAA
R TTC CCG AGG TCC ATC TAC TGT AAC TT	R TCTCCCACAACACATAACTTCG
hCD44 (for qRT-PCR)	*mWnt9b for qRT-PCR*
F AAA GGA GCA GCA CTT CAG GAG GTT AC	F CTCCAGAGAGGCTTTAAGGAGAC
R CTG TCT GTG CTG TCG GTG ATC CAG GG	R GGGAGTCGTCACAAGTACAGC
mCd44 (for qRT-PCR)	*mPtpqr (for qRT-PCR)*
F AAG TCT TCC CAC AGA TAC AAC TAC TTC	F CGGAGGTTACTGGAACCGTG
R AGT CAG TAG CAA GAG TCA CTT CAG TTT	R CAGGGTCCCCACATAGCCT

hAXIN2 (for qRT-PCR)	*hGAPDH (for ChIP)*
F CTC CTT GGA GGC AAG AGC	F CGGCTACTAGCGGTTTTACG
R GGC CAC GCA GCA CCG CTG	R AAGAAGATGCGGCTGACTGT
mAxin2 (for qRT-PCR)	*mS18 (for qRT-PCR)*
F GTG GAC CAA GTC TTT ACA CTC CTT	F AAG TCC CTG CCC TTT GTA CAC A
R GTT TTG GTA TCC TTC AGG TTC ATC	R GAT CCG AGG GCC TCA CTA AAC
hHPRT1 (for qRT-PCR)	*hTBX3 for (qRT-PCR)*
F GCT ATA AAT TCT TTG CTG ACC TGC TG	F AAAGAACTTTGGGATCAGTTTCAC
R AAT TAC TTT TAT GTC CCC TGT TGA CTG G	R ATCAGCAGCTATAATGTCCATCAA
mCcnd1 (for qRT-PCR)	
F GCGTACCCTGACACCAATCTC	
R CTCCTCTTCGCACTTCTGCTC	